

# ASSESSING THE STRESS FIELDS IN AN INJECTION-MOULDED UNDERCUT GEOMETRY DURING EJECTION SUPPORTED BY NEURAL NETWORKS

## MODEL NAPOVEDOVANJA NAPETOSTI V OBMOČJU ZASKOČNE GEOMETRIJE TERMOPLASTIČNEGA IZDELKA Z NEVRONSKIMI MREŽAMI

**Blaž Florjanič<sup>1</sup>, Uroš Božič<sup>1</sup>, Boštjan Zafošnik<sup>2</sup>**

<sup>1</sup>University of Ljubljana, Faculty of Mechanical Engineering, Aškerčeva 6, 1000 Ljubljana, Slovenia

<sup>2</sup>School of Technologies and Systems, VITEŠ, Na Loko 2, 8000 Novo mesto, Slovenia  
info@imold.si

*Prejem rokopisa – received: 2013-09-30; sprejem za objavo – accepted for publication: 2013-10-29*

The continuous demand for cost optimization in the manufacturing of thermoplastic polymer products leads to the design trend of minimizing the number of assembly parts, which consequentially increases their geometrical complexity. This trend directly influences the manufacturing process of injection-moulded thermoplastic polymer parts. Parts designed in accordance with this design trend have many undercut-geometry features, which usually cannot be ejected from the mould without complex mould kinematics. A typical case of undercut geometry is represented by an annular snap joint, which can be released from the mould core by stripping it off. Stripping it off can be applied if the undercut geometry is deformed within the material's elasticity limits during ejection. When the stripping-off principle is used, an analysis of the stress field in the area of the product's undercut geometry should be carried out. Finite-element methods are commonly applied for determining the stress field. These methods offer a single point solution that requires lots of engineering effort and has to be repeated for any geometry modification. This study is focused on developing an artificial-neural-network response model that properly describes the relationships between the input factors (geometrical features) and the corresponding responses (maximum stress) in an undercut area. To overcome the necessity of carrying out numerical simulations for all the input-factor combinations the Taguchi design of experiment was used. Both the analysis of variance performed within the Taguchi design of experiment and the artificial neural network model validation confirmed that the most influential geometrical input factor is the draft angle. For the artificial-neural-network model validation a virtual full-factorial design of experiment was used and the response surfaces were generated based on the obtained experimental results. Although the model solution is developed for a specific undercut geometry, the presented paper offers a generalized approach for assessing the stress field of the undercut-geometry features.

Keywords: thermoplastic polymers, injection moulding, finite-elements method, design of experiments, artificial neural networks

Stalna zahteva globalne ekonomije po optimizaciji stroškov v proizvodnji izdelkov iz termoplastičnih polimerov potiska v ospredje zahtevo po zmanjšanju števila montažnih delov, kar posledično pomeni povečanje njihove geometrijske kompleksnosti. Ta usmeritev neposredno vpliva tudi na proizvodni proces injekcijskega brizganja termoplastičnih polimerov. Sestavni deli, konstruirani v skladu s to usmeritvijo, imajo veliko geometrijskih področij z negativnimi snemalnimi koti, zaradi katerih je treba v orodjih uporabiti mehanizme s kompleksno kinematiko. Eden osnovnih primerov je cilindrična zaskočna geometrija, ki jo je mogoče izmetati s prisilnim snemanjem. Princip prisilnega snemanja geometrije izdelka je mogoče uporabiti kadar se geometrija z negativnimi snemalnimi koti med izmetavanjem poda v okviru meja elastične deformacije. Pri apliciranju prisilnega snemanja je priporočljivo izvesti analizo napetosti, za kar se navadno uporablja metoda končnih elementov. Ta metoda je časovno potratna, zahteva veliko inženirskih in procesorskih virov ter jo je treba ponoviti ob kakršni koli spremembi vhodnih podatkov. Predstavljena raziskava obravnava razvoj modela z uporabo umetnih nevronske mreže, ki ustrezno obravnava odnose med vhodnimi spremenljivkami (geometrijske karakteristike) in pripadajočim odzivom (maksimalno napetostjo) v območju geometrije z negativnimi snemalnimi koti. Da bi se odpravila potreba po izvajanju obsežnega števila analiz z metodo končnih elementov, je bilo izvedeno načrtovanje eksperimenta po Taguchijevi metodi. Tako analiza variance rezultatov eksperimenta, kot tudi validacija modela, podprtega z nevronske mreže, sta potrdili, da je najbolj vplivna geometrijska spremenljivka snemalni kot izdelka. Za presojo vplivnosti posamezne vhodne spremenljivke modela, podprtega z nevronske mreže, je bilo izvedeno virtualno načrtovanje eksperimenta, pridobljeni rezultati pa so bili podlaga za oblikovanje odzivnih površin. Predstavljena raziskava ponuja generaliziran način za hitro oceno napetostnega polja v polimernih izdelkih, ki je bil preverjen pri značilnem primeru zaskočne geometrije.

Ključne besede: termoplastični polimeri, injekcijsko brizganje, metoda končnih elementov, načrtovanje eksperimentov, nevronske mreže

## 1 INTRODUCTION

Undercuts can be defined as the geometrical features on an injection-moulded part whose projection lines in the direction of a mould-opening vector overlap the geometry of the same part. Undercuts prevent the moulded parts from being removed from the cavity in an axial direction and are said to create a die-lock situation.<sup>1</sup>

These require the use of special mould features such as side cores, split cavities, collapsible cores, unscrewing devices, or stripper plates.<sup>2</sup> Some undercuts, like the snap rings on many container caps, can be stripped off the core forming it.<sup>2</sup> This means pushing the thermoplastic material out of the grooves that prevent the product from easily pulling off the core. This method is very

common but depends on the shape of the grooves and the types of thermoplastic material.<sup>3</sup> The allowable deformation should not be exceeded during the ejection of the part from the mould.<sup>4</sup> Only somewhat elastic thermoplastic polymer materials can be stripped, typically polyethylene (PE) and polypropylene (PP). Occasionally, even thermoplastic materials with a lower elasticity such as polystyrene (PS) can be stripped, if the amount of deformation during stripping is within the elastic limit at the temperature given at the moment of ejection.<sup>3</sup>

In this study the special case of an undercut geometry, called an annular snap joint, was observed (**Figure 1**). The following geometrical features were observed as the input factors: draft angle ( $\beta$ ), inner radius ( $R$ ), and thickness ( $t$ ). The thermoplastic polymer material used for the observed part is polyester-based grade BASF Elastollan® C85A.

Artificial neural networks (ANNs) are recognized as universal function approximators and can be efficiently used to model high-dimensional and nonlinear relations.<sup>5</sup> In order to generate and validate the ANN model the research was carried out with the following steps:

1. Definition of the observed input factors
2. Taguchi Design of Experiment (DOE) preparation
3. Numerical simulations of stress field using finite-element methods (FEMs) and retrieval of the maximum stress
4. Experiment result analysis
5. ANN modelling and response validation
6. Deploying virtual full-factorial DOE on ANN model and response surface generation

## 2 EXPERIMENT PREPARATION

The experiment preparation includes the input variable definition, the Taguchi DOE, and the CAD model generation.

The correct approach to dealing with several factors is to conduct a factorial experiment.<sup>6</sup> For three observed

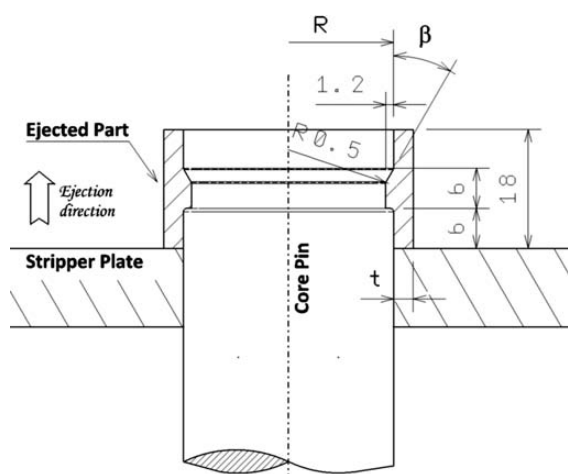


Figure 1: Annular snap joint

Slika 1: Cilindrična zaskočna nerazstavljava zveza

factors ( $\beta$ ,  $R$ , and  $t$ ) four levels were defined, as shown in **Table 1**. To cover all the variable combinations on all levels  $4^3 = 64$  runs would be carried out. This represents a full-factorial DOE. Since the FEM requires extended engineering resources, a reduced optimized number of runs was achieved by using the L16 Taguchi Orthogonal Array DOE, as shown in **Table 2**.

Table 1: DOE controllable factor levels

Tabela 1: Nivoji spremenljivk za načrtovani eksperiment

Controllable factors	Level 1 (Low)	Level 2 (Middle)	Level 3 (High)	Level 4 (High+)
Draft Angle $\beta/^\circ$	30	40	50	60
Inner radius $R/\text{mm}$	10	13	16	19
Thickness $t/\text{mm}$	2.5	3	3.5	4

The product CAD data was generated with CATIA V5 R19 software.

## 3 FEM NUMERICAL SIMULATIONS AND RETRIEVAL OF THE MAXIMUM STRESS

This study deals with several nonlinearities: contact, material, and geometrical.<sup>7</sup> All the mentioned nonlinearities can be captured with the finite-element method (FEM). It was considered that the ejection of a moulded part is performed at 100 °C, and that there is a good lubrication between the ejected part and the core pin, which reduces the coefficient of friction to  $\approx 0$ . Due to the high temperature the strain rate has a very small influence on the stress-strain behaviour of the BASF Elastollan® C85A. This property was determined with extra experimental testing using a high-speed testing device. The Marlow constitutive model<sup>8</sup> was used to model the stress-strain behaviour during ejection. The annular snap joint in **Figure 1** presents a cylindrical geometry, and so

Table 2: Experiment results, L16 Taguchi DOE

Tabela 2: Rezultati eksperimenta, L16 Taguchijeva metoda

Run No.	Controllable factors			FEM Response Maximum Stress	S/N-value
	$\beta/^\circ$	$R/\text{mm}$	$t/\text{mm}$	$\sigma_{\text{max}}/\text{MPa}$	
1	30	10	2.5	1.707	-4.645
2	30	13	3	1.722	-4.721
3	30	16	3.5	1.754	-4.881
4	30	19	4	1.718	-4.700
5	40	10	3	2.205	-6.868
6	40	13	2.5	1.908	-5.612
7	40	16	4	2.020	-6.107
8	40	19	3.5	1.770	-4.959
9	50	10	3.5	2.595	-8.283
10	50	13	4	2.408	-7.633
11	50	16	2.5	1.869	-5.432
12	50	19	3	1.895	-5.552
13	60	10	4	2.813	-8.983
14	60	13	3.5	2.528	-8.056
15	60	16	3	2.233	-6.978
16	60	19	2.5	1.880	-5.483

an axisymmetric numerical model can be used. The stripper plate and the core pin (**Figure 1**) were modelled as analytical rigid parts because they have a much higher stiffness than the ejected part, which was discretized with 4-noded, bilinear, axisymmetric quadrilateral elements using hourglass control and reduced integration. The calculation was made using an Explicit solver.<sup>8</sup> The core pin was fixed and the stripper plate was controlled with a constant velocity of 20 mm/s.

**Table 2** presents the results for the maximum von Mises stress that occurs in the undercut geometry during ejection.

The results in **Table 2** show that the highest von Mises stress occurs for Run No.13, where  $\beta = 60^\circ$ ,  $R = 10$  mm and  $t = 4$  mm.

The results in **Figure 2** show that the highest stress in the ejected part occurs below the surface in the region of contact between the fillets of the ejected part and the core pin.



**Figure 2:** Stress field ( $\beta = 40$  mm,  $R = 10$  mm,  $t = 3$  mm)

**Slika 2:** Napetostno polje ( $\beta = 40$  mm,  $R = 10$  mm,  $t = 3$  mm)

#### 4 ANALYSIS OF THE EXPERIMENTAL RESULT

Design of experiments is an effective approach to optimizing the throughput in various manufacturing-related processes.<sup>9</sup> In this study the Taguchi DOE was used (**Table 2**). Three geometry variables,  $\beta$ ,  $R$ , and  $t$ , were studied at four levels. MINITAB 16 software was used to design the simulations and to model and analyse the results. The summary statistics  $S/N$  signal-to-noise ratios were calculated based on the following equation:

$$S/N_i = -10 \lg \sigma_i^2 \quad (1)$$

where  $\sigma_i^2$  is the square stress value of the  $i$ -th dataset. The dataset combinations that were numerically analysed with the computed stress values and  $S/N$  statistics are shown in **Table 2**.

The effect of the factor is defined as the response change from the overall mean due to a change in the

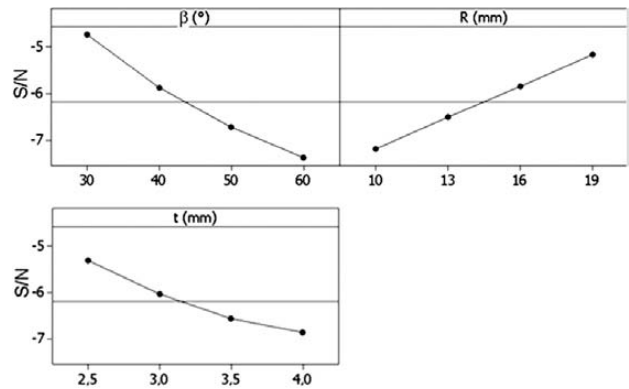


**Figure 3:** Main separate effects plot for each factor  $S/N$  values

**Slika 3:** Diagram vplivnosti  $S/N$ -vrednosti posameznega faktorja

level of that factor. The main effect plot was used to analyse the importance of the factors in **Figure 3**.

The important goal in the matrix experiment is to find the optimum level for each factor. The Taguchi methodology defines three types of quality characteristics, which are the-smaller-the-better, the-larger-the-better, and the-nominal-the-best. The design of the injection-moulding geometry should take steps towards reducing the stress values inside the moulding during ejection. Therefore, a smaller-the-better quality characteristic is implemented in this study, which means that we should maximize the  $S/N$  values because of a decreasing function – log. It was determined in **Figure 3** by observing the optimum level for each factor at the highest value of  $S/N$ . Thus, the optimum draft angle is  $\beta$  ( $30^\circ$ ), the optimal inner radius is  $R$  (19 mm), and the optimal thickness is  $t$  (2.5 mm). The predicted best setting does not correspond to one of the runs in the matrix, which is normal. The average  $S/N$  for each level of the three factors is listed in **Table 3**. These averages, known as main effects, are also shown in **Figure 3**.

**Table 3:** Average  $S/N$  ratio by factor levels with an overall mean of  $-6.18$

**Tabela 3:** Povprečni  $S/N$  za posamezni nivo spremenljivke (skupno povprečje  $-6,18$ )

Controllable factors	Average S/N ratio			
	Level 1	Level 2	Level 3	Level 4
Draft Angle $\beta/^\circ$	-4.74	-5.89	-6.73	-7.37
Inner radius $R/\text{mm}$	-7.19	-6.51	-5.85	-5.17
Thickness $t/\text{mm}$	-5.29	-6.03	-6.54	-6.86

#### 4.1 Analysis of variance

The purpose of ANOVA is to determine the relative importance of the geometry factors on the process output. **Table 4** shows the ANOVA results. The sum of squares due to the factors  $\beta$ ,  $R$ ,  $t$  are, respectively, 15.33, 9.03, and 5.42. Thus, the factor  $\beta$  represents a major portion of the total variation of the  $S/N$ . In other words, factor  $\beta$  is responsible for  $(15.33/30.64) \times 100 = 50.03\%$  of the  $S/N$  variation. This result is followed by two other

factors, factor  $R$  with next largest portion, i.e., 29.47 %, and factor  $t$  with 17.69 % of the variation in  $S/N$ . The smallest portion of the variation goes to the error term that explains 2.84 % of the variation. The ANOVA also indicates that all three factors are highly significant since their  $F$  values (35.17, 20.72, and 12.43) are high compared to  $F_{0.05,3,15} = 3.29$ .

**Table 4:** Analysis of Variance  
**Tabela 4:** Analiza variances

Source	DF	SS	MS	F
Draft Angle $\beta/^\circ$	3	15.33	5.11	35.17
Inner radius $R/\text{mm}$	3	9.03	3.01	20.72
Thickness $t/\text{mm}$	3	5.42	1.81	12.43
Residual Error	6	0.87	0.15	
Total	15	30.64		

NOTES: DF... Degrees of freedom, SS... Sum of squares, MS... Mean squares, F... statistic

#### 4.2 Prediction of $S/N$ under optimal conditions

The principal goal of conducting Robust Design experiments is to determine the optimum level of each factor. In this study the optimum condition is  $\beta$  ( $30^\circ$ ),  $R$  (19 mm), and  $t$  (2.5) mm. The additive model<sup>10</sup> to predict the value of the  $S/N$  ratio under the optimum conditions was used:

$$\frac{S}{N_{opt}} = m + b_i + R_j + t_k + e$$

$$\frac{S}{N_{opt}} = -6.18 + (-4.74 + 6.18) + (-5.17 + 6.18) + (-5.29 + 6.18) \quad (2)$$

$$\frac{S}{N_{opt}} = -2.84$$

where  $m$  is the overall mean of the  $S/N$  for the experimental region, and  $\beta_i$ ,  $R_j$ ,  $t_k$  are deviations from  $m$  caused by the factors  $\beta$ ,  $R$ , and  $t$ , respectively. The term  $e$  indicates the error. Since the sum of squares due to the error is small, the corresponding contribution was removed in the prediction of the  $S/N$  under optimum conditions. The values in Eq. (2) are taken from **Table 3**.

Using Eq. (1) the stress value under the optimum conditions was predicted as:

$$\sigma = \sqrt{10^{\frac{-S/N_{opt}}{10}}} = \sqrt{10^{0.284}} = 1.387 \text{ MPa} \quad (3)$$

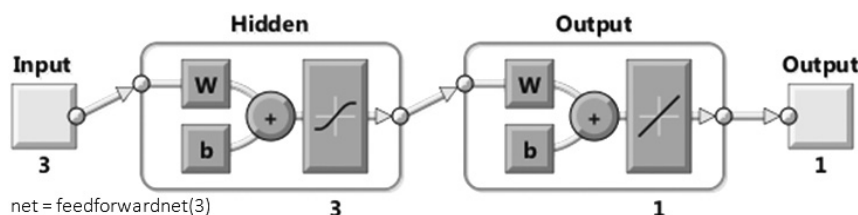


**Figure 4:** ANN architecture generated with MATLAB

**Slika 4:** Arhitektura nevronske mreže, generirane v programskem okolju MATLAB

#### 4.3 Confirmation simulation

After the calculation of the optimal conditions a numerical simulation with optimum parameter settings was performed. The simulation output with the prediction was compared. The simulation output under  $\beta$  ( $30^\circ$ ),  $R$  (19 mm), and  $t$  (2.5 mm) yields 1.399 MPa, which is very close to the predicted stress of 1.387 MPa, as calculated in Eq. (3). Having simulated and predicted values close to each other, it can be concluded that the additive model is adequate for describing the dependence of the  $S/N$  ratio on the various parameters.

#### 5 ANN MODEL FOR ASSESSING THE MAXIMUM STRESS

ANNs provide non-parametric, data-driven, self-adaptive approaches to information processing.<sup>11</sup> To model a multivariable relation between the selected variable factors and the corresponding maximum stress a multi-layer, feed-forward network was used. The multi-layer feed-forward neural networks are usually applied for function-fitting problems. For ANN model generation a MATLAB 7.11.0.584 (R20130b) software environment was used. In order to avoid over fitting a simple, two-layer, feed-forward network was created using the Neural Network Toolbox™. Feed-forward networks often have one or more hidden layers of sigmoid neurons followed by an output layer of linear neurons. Multiple layers of neurons with nonlinear transfer functions allow the network to learn nonlinear relationships between the input and output vectors. The linear output layer is most often used for function fitting (or nonlinear regression) problems.<sup>12</sup> There are several training algorithms that can be used, from among which the Levenberg-Marquard back-propagation algorithm was adopted. It is a method that is normally used for small and medium-sized feed-forward neural networks.<sup>12</sup>

As a performance function for feed-forward networks a mean square error ( $MSE$ ) was used, which defines the average squared difference between the network outputs and the target responses.

Through an iteration process of testing several feed-forward ANN architectures an optimised solution was chosen, as shown in **Figure 4**. It has 3 units in the input layer, 3 neurons with a sigmoid activation function in the hidden layer, and a single output neuron with a linear activation function.

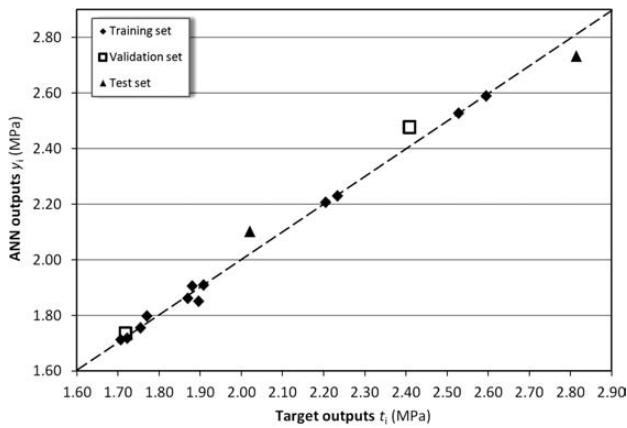


**Figure 5:** Scatter plot of ANN outputs vs. target outputs  
**Slika 5:** Diagram raztrosa odzivov modela, podprtega z nevronska mrežo

The ANN model results are shown in **Table 5**. The training set returned a root mean square error (*RMSE*) of 0.017 MPa and a mean absolute percentage error (*MAPE*) of 0.07 %. Both the validation set and the test set show an acceptable root mean square error (*RMSE*) of 0.052 MPa and 0.082 MPa, and also low mean absolute percentage errors (*MAPE*) of 2.06 % and 0.67 %. These results show an acceptable level of ANN model performance. Confirmation of this conclusion is also a low scatter between the target value and the corresponding ANN response, shown in **Figure 5**. All the datasets show high correlation coefficients.

**Table 5:** ANN model results

**Tabela 5:** Odziva modela

	Training set	Validation set	Test set	All
<i>RMSE</i> /MPa	0.017	0.052	0.082	0.037
<i>MAPE</i> /%	0.07	2.06	0.67	1.14
Correlation coefficient	0.99829	1	1	0.99442

$$RMSE = \sqrt{\frac{1}{N} \sum_{i=1}^N (t_i - y_i)^2} \quad (4)$$

**Table 7:** Analysis of Variance for  $\sigma_{max}$ /MPa

**Tabela 7:** Analiza variance za napetost  $\sigma_{max}$ /MPa

Source	DF	Seq SS	Adj SS	Adj MS	F	P
Draft Angle $\beta/^\circ$	3	3.46610	3.46610	1.15537	620.96	0.000
Inner radius <i>R</i> /mm	3	2.15679	2.15679	0.71893	386.39	0.000
Thickness <i>t</i> /mm	3	1.38575	1.38575	0.46192	248.26	0.000
$\beta * R$	9	0.07428	0.07428	0.00825	4.44	0.001
$\beta * t$	9	0.00542	0.00542	0.00060	0.32	0.960
$R * t$	9	0.00304	0.00304	0.00034	0.18	0.994
Residual Error	27	0.05024	0.05024	0.00186		
Total	63	7.14161				

S = 0.0431350 R-Sq = 99.30 % R-Sq(adj) = 98.36 %

NOTES: DF... Degrees of freedom, Seq SS... Sequential sums of squares, Adj SS... Adjusted sums of squares, Adj MS... Adjusted mean squares, F... statistic, P... Probability, S... Estimate of the variance, R-Sq... Coefficient of determination, R-Sq(adj)... Modified R-Sq that has been adjusted for the number of terms in the model

$$MAPE = \frac{1}{N} \sum_{i=1}^N \left| \frac{t_i - y_i}{t_i} \right| \quad (5)$$

In the above equations  $t_i$  and  $y_i$  denote the target and the ANN response and  $N$  denotes the number of input samples.

Because of the small sample set a further ANN model verification was carried out on an additional three test samples, which were not included in neural network generation. The test sample data is shown in **Table 6**. The ANN model responses were observed and compared with the FEM responses. The calculated relative percentage error (*RPE*) confirms that the ANN responses are within an acceptable accuracy.

**Table 6:** ANN model verification

**Tabela 6:** Ovrednotenje odziva modela

Verification Run No.	Controllable factors			Response $\sigma_{max}$ /MPa		<i>RPE</i> /%
	$\beta/^\circ$	<i>R</i> /mm	<i>t</i> /mm	FEM	ANN	
1	35	17	3.2	1.798	1.731	-3.75
2	42	14	3.7	2.229	2.186	-1.91
3	53	12	2.8	2.290	2.333	-1.87

*RMSE* = 0.052 MPa      *MAPE* = 1.62 %

## 6 VIRTUAL DOE AND RESPONSE SURFACE GENERATION

To identify the significance of the input factors ( $\beta$ , *R* and *t*) and their interactions ( $\beta * R$ ,  $\beta * t$  and  $R * t$ ) in the ANN model a full-factorial DOE ( $4^3 = 64$  runs) was carried out, with the levels defined in **Table 1**. A full-factorial design was used, because the virtual environment in this case does not represent resource limitations, and there was no necessity to use any of the fractional factorial design at disposal. The analysis of variance shown in **Table 7** indicates that all the input factors can be considered significant, because their P-value is below a threshold of 0.05. On the other hand, their interactions cannot be considered as significant except for  $\beta * R$ .

To analyse the importance of the input factors in the ANN model, the main effect plot was generated as

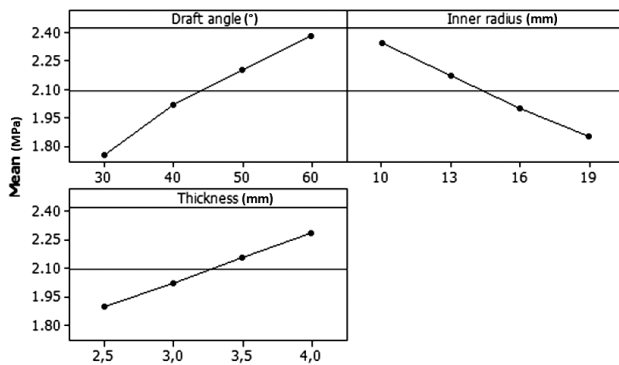


Figure 6: Main effects plot for  $\sigma_{\max}$ /MPa

Slika 6: Diagram vplivnosti faktorjev na napetost  $\sigma_{\max}$ /MPa

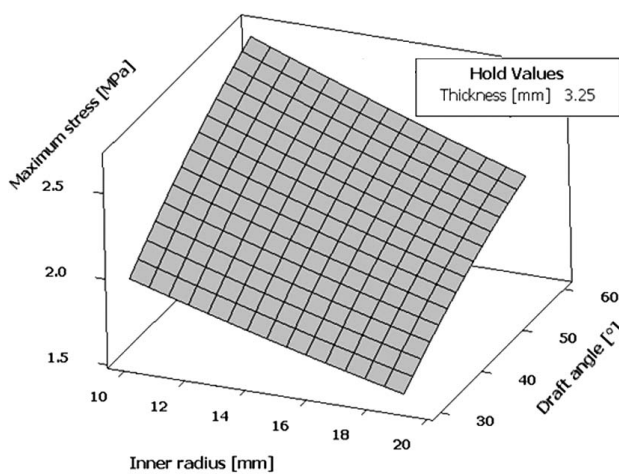


Figure 7: Response-surface plot for  $\sigma_{\max}$ /MPa

Slika 7: Diagram odzivne površine za napetost  $\sigma_{\max}$ /MPa

shown in **Figure 6**. From the plot it can be concluded that the most significant input factor is the draft angle ( $\beta$ ), followed by the inner radius ( $R$ ) and the thickness ( $t$ ). While the draft angle ( $\beta$ ) and the thickness ( $t$ ) have positive gradients, the inner radius ( $R$ ) shows that with increasing value the maximum stress decreases.

To properly visualize the effect of the two most influential input factors' responses, surface modelling was applied to the developed ANN model. **Figure 7** shows the predicted maximum stress at a fixed thickness of 3.25 mm. As expected, the surface response confirms the already observed gradients in the main effect plot as shown in **Figure 6**.

## 7 DISCUSSION AND CONCLUSIONS

This paper proposes an implementation and evaluation of an ANN-based model for assessing the stress field in an injection-moulded undercut geometry during ejection at an acceptable accuracy level. The stress field

in the injection-moulded undercut geometry was determined with a finite-element model, where besides contact also material and geometrical nonlinearities were considered. Both the analyses of variance performed on the Taguchi DOE and ANN model validation, carried out through separate statistical analyses, confirmed that all the observed input factors draft angle ( $\beta$ ), inner radius ( $R$ ), and thickness ( $t$ ) can be considered statistically significant. While an increased draft angle ( $\beta$ ) or thickness ( $t$ ) means a higher maximum stress, an increased inner radius ( $R$ ) reduces it.

The following benefits can be expected by applying the proposed approach:

- Structured methodology for generating and evaluating an ANN-based stress-assessment model;
- Reduction of engineering efforts for maximum stress assessment when high geometrical variability is considered;
- Better understanding of input factors influence on the maximum stress.

The proposed solution for generating and evaluating an ANN-based stress-assessment model can be used as a generalized solution approach and expanded to similar cases.

## 8 REFERENCES

- <sup>1</sup> G. Boothroyd, P. Dewurst, W. A. Knight, Product Design for Manufacture and Assembly, Third Edition, CRC Press, Boca Raton 2011
- <sup>2</sup> T. A. Osswald, L. S. Turng, P. Gramann, Injection Molding Handbook, 2<sup>nd</sup> Edition, Hanser Gardner Publications, 2008
- <sup>3</sup> H. Rees, Mold Engineering, 2<sup>nd</sup> Edition, Hanser Gardner Publications, 2011
- <sup>4</sup> Snap-Fit Joints for Plastic – A Design Guide, Bayer Material Science, MS 00062550, Edition 02 / 2013, www.plastics.bayer.com
- <sup>5</sup> S. Cavalier, P. Maccarone, R. Pinto, Parametrical vs. Neural Network Models for Estimation of Product Costs: A Case Study in the Automotive Industry, International Journal of Production Economics, (2004) 91, 165–177
- <sup>6</sup> D. C. Montgomery, Design and Analysis of Experiment, 8<sup>th</sup> Edition, John Wiley & Sons, 2013
- <sup>7</sup> NAFEMS, Introduction to Nonlinear Finite Element Analysis, Glasgow, 1991
- <sup>8</sup> ABAQUS, Version 6.12-1 documentation, 2012
- <sup>9</sup> B. Ozcelik, T. Erzurumlu, Comparison of the Warpage Optimization in the Plastic Injection Molding using ANOVA, Neural Network Model and Genetic Algorithm, Journal of Materials Processing Technology, 171 (2006), 437–445
- <sup>10</sup> M. S. Phadke, Quality Engineering Using Robust Design, AT&T Bell Laboratories, USA, 1989
- <sup>11</sup> X. Shi, P. Schillings, D. Boyd, Applying Artificial Neural Networks and Virtual Experiment Design to Quality Improvement of Two Industrial Processes, International Journal of Production Research, 42 (2004) 1, 101–118
- <sup>12</sup> M. H. Beale, M. T. Hagan, H. W. Demuth, MATLAB, Neural Network Toolbox™ 7, User's Guide, online edition, The MathWorks, Inc., 2010